

JET TOMOGRAPHY IN HEAVY ION COLLISIONS

URS ACHIM WIEDEMANN

CERN TH Division, CH-1211 Geneva 23

E-mail: Urs.Wiedemann@cern.ch

We review recent calculations of the probability that a hard parton radiates an additional energy fraction ΔE due to scattering in spatially extended matter, and we discuss their application to the suppression of leading hadron spectra in heavy ion collisions at collider energies.

1. Introduction

Experiments at the Relativistic Heavy Ion Collider RHIC in Brookhaven show for the first time a significant quenching of high- p_\perp leading hadron spectra. In particular, transverse momentum spectra for neutral pion^{1,2} and charged hadron^{1,3} are suppressed if compared to spectra in p+p collisions rescaled by the number of binary collisions. This suppression is most pronounced (up to a factor ~ 5) in central Au+Au collisions and smoothly approaches the binary scaling case with decreasing centrality. The azimuthal anisotropy $v_2(p_\perp)$ of hadroproduction stays close to maximal up to the highest transverse momentum⁴. Moreover, the disappearance of back-to-back high- p_\perp hadron correlations⁵ provides an additional indication that final state medium effects play a decisive role in hadroproduction up to $p_\perp \sim 10$ GeV.

Parton energy loss has been proposed to account for the small nuclear modification factor⁶, the azimuthal anisotropy⁷ and the disappearance of dijets^{8,9}. Several studies (see references given in¹⁰) indicate, however, that in the kinematical regime relevant for RHIC ($p_\perp < 12$ GeV), p_\perp -broadening, shadowing, formation time and possibly other effects contribute significantly to the high- p_\perp nuclear modification as well.

Here, we discuss the status of parton energy loss calculations and their comparison to data in the kinematical p_\perp -range probed at RHIC.

2. Medium-induced gluon radiation from a static medium

Several groups ^{11,12,13,14} calculated recently the modification of the elementary splitting processes $q \rightarrow qg$ and $g \rightarrow gg$ due to multiple scattering. The inclusive energy distribution of gluon radiation off an in-medium produced parton takes the form ^{13,15}

$$\omega \frac{dI}{d\omega} = \frac{\alpha_s C_R}{(2\pi)^2 \omega^2} 2\text{Re} \int_{\xi_0}^{\infty} dy_l \int_{y_l}^{\infty} d\bar{y}_l \int d^2\mathbf{u} \int_0^{\chi\omega} d^2\mathbf{k} e^{-i\mathbf{k}_\perp \cdot \mathbf{u}} e^{-\frac{1}{2} \int_{\bar{y}_l}^{\infty} d\xi n(\xi) \sigma(\mathbf{u})} \times \frac{\partial}{\partial \mathbf{y}} \cdot \frac{\partial}{\partial \mathbf{u}} \int_{\mathbf{y}=0}^{\mathbf{u}=\mathbf{r}(\bar{y}_l)} D\mathbf{r} \exp \left[i \int_{y_l}^{\bar{y}_l} d\xi \frac{\omega}{2} \left(\dot{\mathbf{r}}^2 - \frac{n(\xi) \sigma(\mathbf{r})}{i\omega} \right) \right], \quad (1)$$

where gluons of transverse momentum $k_\perp < \chi\omega$ are included. The radiation of hard quarks or gluons differs by the Casimir factor $C_R = C_F$ or C_A , respectively. The properties of the medium enter eq. (1) by the product of the time-dependent density $n(\xi)$ of scattering centers times the strength of a single elastic scattering $\sigma(\mathbf{r}) = 2 \int \frac{d\mathbf{q}}{(2\pi)^2} |a(\mathbf{q})|^2 (1 - e^{i\mathbf{q} \cdot \mathbf{r}})$, where $|a(\mathbf{q})|^2$ denotes the elastic high-energy cross section of a single scatterer.

For explicit calculations, one has to approximate the path integral in (1). This is done either by a saddle point approximation ¹² obtained in the medium-induced soft multiple scattering approximation,

$$n(\xi) \sigma(\mathbf{r}) \simeq \frac{1}{2} \hat{q}(\xi) \mathbf{r}^2. \quad (2)$$

Here, the only medium-dependent quantity is the transport coefficient ¹⁶ $\hat{q}(\xi)$ which characterizes the transverse momentum squared μ^2 transferred to the projectile per mean free path λ . Alternatively, one can proceed in the opacity expansion which amounts to expanding the path integral in (1) in powers of the elastic scattering center ^{13,14}

$$K(\mathbf{r}, y_l; \bar{\mathbf{r}}, \bar{y}_l) = D\mathbf{r} \exp \left[i \int_{y_l}^{\bar{y}_l} d\xi \frac{\omega}{2} \left(\dot{\mathbf{r}}^2 - \frac{n(\xi) \sigma(\mathbf{r})}{i\omega} \right) \right] \quad (3)$$

$$= K_0(\mathbf{r}, y_l; \bar{\mathbf{r}}, \bar{y}_l) - \int_z^{z'} d\xi n(\xi) \int d\rho K_0(\mathbf{r}, y_l; \rho, \xi) \frac{\sigma(\rho)}{2} K_0(\rho, \xi; \bar{\mathbf{r}}, \bar{y}_l) + \dots$$

Fig.1 compares numerical results for the gluon energy distribution obtained in these two approximations. Qualitatively, this figure can be understood by estimating to what degree initial state gluons *decohere* from the partonic projectile. Decoherence depends on the relative phase φ accumulated by the gluon due to scattering. This phase grows with the transverse momentum accumulated by the emitted gluon.

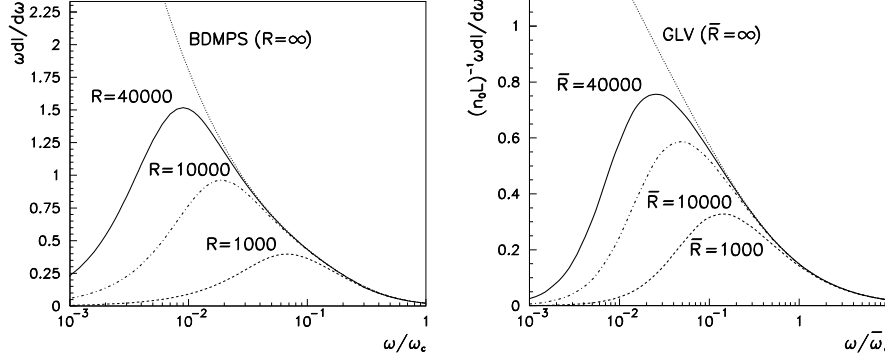


Figure 1. The gluon energy distribution in the multiple soft (LHS) and single hard (RHS) scattering approximation calculated for different values of the kinematical constraints R , \bar{R} respectively. Fig. from Ref.¹⁰.

For multiple soft scattering, we have¹⁷

$$\varphi = \left\langle \frac{k_{\perp}^2}{2\omega} \Delta z \right\rangle \sim \frac{\hat{q} L}{2\omega} = \frac{\omega_c}{\omega}, \quad (4)$$

which defines the “characteristic gluon frequency” $\omega_c = \frac{1}{2} \hat{q} L^2$. Given the number N_{coh} of scattering centers which add coherently in the gluon phase (4), one find $k_{\perp}^2 \simeq N_{\text{coh}} \mu^2$. With the coherence time of the emitted gluon, $t_{\text{coh}} \simeq \frac{\omega}{k_{\perp}^2} \simeq \sqrt{\frac{\omega}{\hat{q}}}$ and $N_{\text{coh}} = \frac{t_{\text{coh}}}{\lambda} = \sqrt{\frac{\omega}{\mu^2 \lambda}}$, one estimates for the gluon energy spectrum per unit pathlength

$$\omega \frac{dI^{(mult)}}{d\omega dz} \simeq \frac{1}{N_{\text{coh}}} \omega \frac{dI^{1\text{scatt}}}{d\omega dz} \simeq \frac{\alpha_s}{t_{\text{coh}}} \simeq \alpha_s \sqrt{\frac{\hat{q}}{\omega}}. \quad (5)$$

This $1/\sqrt{\omega}$ -energy dependence agrees with the small- ω behaviour in Fig.1. It is cut off for $\omega > \omega_c$ where the phase (4) is smaller than unity and the reduced decoherence suppresses gluon emission.

For single hard scattering ($N = 1$ opacity expansion) with momentum transfer μ , decoherence occurs if the typical gluon formation time $\bar{t}_{\text{coh}} = \frac{2\omega}{\mu^2}$ is smaller than the typical distance L between the production point of the parton and the position of the scatterer. The relevant phase is

$$\gamma = \frac{L}{\bar{t}_{\text{coh}}} \equiv \frac{\bar{\omega}_c}{\omega}, \quad (6)$$

which defines the characteristic gluon energy $\bar{\omega}_c = \frac{1}{2}\mu^2 L$. The gluon energy spectrum per unit pathlength can be estimated in terms of the coherence time \bar{t}_{coh} ,

$$\omega \frac{dI^{N=1}}{d\omega dz} \simeq \frac{\alpha_s}{\bar{t}_{\text{coh}}} \simeq \alpha_s \frac{\mu^2}{\omega}. \quad (7)$$

The full calculation in Fig.1 agrees with this $1/\omega$ -dependence in the range $\omega > \bar{\omega}_c$.

In QCD, collinear gluons are hard and softer gluons tend to be emitted under larger angles. As a consequence, the limitations on transverse momentum phase space translate into a depletion of the infrared region of the gluon energy distribution, seen in Fig.1. The estimates (5) and (7) determine the dependence on the characteristic gluon energies ω_c ($\bar{\omega}_c$) only. They do not include the constraint on transverse phase space. The latter is determined by the parameters¹⁸

$$R_\chi = \frac{1}{2} \hat{q} \chi^2 L^3 = \chi^2 \omega_c L, \quad \bar{R}_\chi = \frac{1}{2} \chi^2 \mu^2 L^2 = \chi^2 \bar{\omega}_c L. \quad (8)$$

Clearly, keeping ω_c ($\bar{\omega}_c$) fixed and taking R (\bar{R}) to infinity amounts to the limit of infinite pathlength. In this limit, the projectile can accumulate an arbitrarily large medium-induced transverse momentum and the limit on transverse momentum phase space is removed. For a medium of finite size, however, gluon emission at angles $\Theta_c^2 \simeq \frac{\langle k_\perp^2 \rangle_{\text{med}}}{\omega^2}$ is suppressed since the emitted gluons are sensitive to the kinematical constraint $k_\perp \leq O(\omega)$. In the multiple soft scattering approximation, this translates into

$$\Theta_c^2 \simeq \frac{\sqrt{\omega \hat{q}}}{\omega^2} \simeq \left(\frac{\omega}{\omega_c} \right)^{-3/2} \frac{1}{R} \sim 1 \implies \frac{\hat{\omega}}{\omega_c} \propto \left(\frac{1}{R} \right)^{2/3}. \quad (9)$$

The position of the maximum of $\omega \frac{dI^{(mult)}}{d\omega}$ as a function of R is consistent with this dependence on $\hat{\omega}$, see Fig. 1.

For the single hard scattering approximation, the corresponding estimate for the infrared cut-off $\hat{\omega}$ due to transverse momentum phase space constraints reads

$$\Theta_c^2 \simeq \frac{\mu^2}{\hat{\omega}^2} \simeq \left(\frac{\bar{\omega}_c}{\hat{\omega}} \right)^2 \frac{1}{R} \sim 1 \implies \frac{\hat{\omega}}{\bar{\omega}_c} \propto \frac{1}{\sqrt{R}}. \quad (10)$$

The position of the maximum of $\omega \frac{dI^{N=1}}{d\omega}$ in Fig. 1 changes $\propto \frac{1}{\sqrt{R}}$, in accordance with this estimate. We thus have a semi-quantitative understanding of how phase space constraints deplete the non-perturbative soft region of the medium-induced gluon energy distribution. This suppression of the

non-perturbative small- ω contributions helps to make the calculation of medium-induced energy loss perturbatively stable.

In Ref.¹⁰, we compare the single hard and multiple soft scattering approximations of (1) in detail. In general, one finds that the gluon energy distribution is significantly harder in the single hard scattering approximation. For example, the average energy loss $\Delta E = \int d\omega \omega \frac{dI}{d\omega}$ receives in the multiple soft scattering approximation a dominant contribution from the region $\omega < \omega_c$. In contrast, the dominant contribution comes from the hard region $\omega > \bar{\omega}_c$ in the single hard scattering approximation.

Remarkably, although both approximations emphasize different kinematical regions, the observable results are quantitatively comparable if comparable sets of model parameters are used. To relate the model parameters in both approximations, one observes that up to logarithmic accuracy $\mu^2 n_0 L \simeq \hat{q} L$, where $n_0 L$ determines the average number of scattering centers within the in-medium pathlength L . This implies

$$R \simeq (n_0 L) \bar{R}, \quad \omega_c \simeq (n_0 L) \bar{\omega}_c. \quad (11)$$

In the multiple soft scattering approximation, one uses the transport coefficient \hat{q} to characterize the average transverse momentum squared per unit pathlength. In the opacity expansion, one specifies not only this information, but additionally the average number of scattering centers in which this momentum transfer takes place. As a consequence, the opacity expansion has one additional model parameter $n_0 L$. Numerically, we find that for the choice $n_0 L = 3$ in (11), the energy density distribution, quenching weight and even the angular dependence of the average energy loss are quantitatively comparable¹⁰. We found deviations from this relation for those quantities for which due to kinematical constraints only the region $\omega < \omega_c$ contributes in *both* approximations, see below. This is in particular the case for the comparison to RHIC data in Fig.4, where $\omega < E < \omega_c$.

3. Quenching Weights

If gluons are emitted independently by a hard parton, then the probability $P(\Delta E)$ that this parton loses an additional energy fraction ΔE can be calculated from the normalized sum of the emission probabilities for an arbitrary number of n gluons which carry away a total energy ΔE :

$$P(\Delta E) = \sum_{n=0}^{\infty} \frac{1}{n!} \left[\prod_{i=1}^n \int d\omega_i \frac{dI(\omega_i)}{d\omega} \right] \delta \left(\Delta E - \sum_{i=1}^n \omega_i \right) \exp \left[- \int d\omega \frac{dI}{d\omega} \right] \quad (12)$$

The summation over arbitrarily many gluon emissions in (12) can be performed analytically by Laplace transformation^{17,18,19}. In general, one finds a discrete and a continuous part,

$$P(\Delta E) = p_0 \delta(\Delta E) + p(\Delta E). \quad (13)$$

The discrete weight p_0 may be viewed as the probability that no additional gluon is emitted due to in-medium scattering and hence no medium-induced energy loss occurs. For finite in-medium pathlength, there is always a finite probability p_0 that the projectile is not affected by the medium. For infinite in-medium pathlength, however, one finds $\lim_{R \rightarrow \infty} p_0 = 0$.

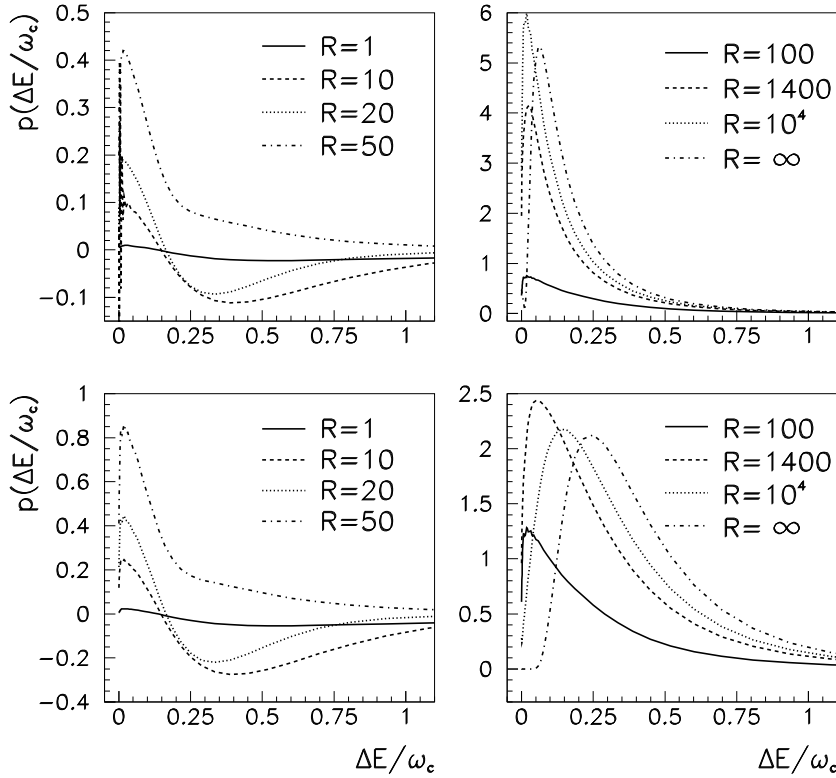


Figure 2. The continuous part of the quenching weight (13), calculated in the multiple soft scattering limit for a hard quark (upper row) or hard gluon (lower row). Fig. from Ref.¹⁰.

In Fig. 2, we show the continuous part of the quenching weight (13) in the multiple soft scattering approximation. The parton energy loss ΔE is

generally seen to increase with increasing characteristic gluon energy ω_c or increasing factor R . This implies that ΔE grows with increasing momentum transfer \hat{q} from the medium, and with increasing in-medium pathlength L , as naively expected.

To understand the negative contributions of the quenching weight for small values R , one recalls that the gluon energy distribution $\omega \frac{dI}{d\omega}$ calculated in (1) is only the medium-induced modification of a radiation pattern $\frac{dI^{(vac)}}{d\omega}$ which occurs in the absence of a medium,

$$\omega \frac{dI^{(tot)}}{d\omega} = \omega \frac{dI^{(vac)}}{d\omega} + \omega \frac{dI}{d\omega}. \quad (14)$$

By writing the corresponding probabilities (11) in Mellin space, one shows that

$$P^{(tot)}(\Delta E) = \int_0^\infty d\bar{E} P(\Delta E - \bar{E}) P^{(vac)}(\bar{E}). \quad (15)$$

The probability $P^{(tot)}(\Delta E)$ is normalized to unity and it is positive definite. In contrast, the medium-induced modification of this probability, $P(\Delta E)$, is a generalized probability. It can take negative values for some range in ΔE , as long as its normalization is unity,

$$\int_0^\infty d\bar{E} P(\bar{E}) = p_0 + \int_0^\infty d\bar{E} p(\bar{E}) = 1. \quad (16)$$

The discrete weight p_0 is found to coincide with this normalization condition. A qualitatively similar behaviour of the quenching weights is found in the single hard scattering approximation.

4. Angular dependence of radiation probability

The quenching weights discussed above allow to calculate the average energy loss *outside* an opening angle Θ ,

$$\begin{aligned} \langle \Delta E \rangle(\Theta) &= \int d\omega \omega \frac{dI^{>\Theta}}{d\omega}(\omega_c, R = \omega_c L) \\ &= \int d\bar{E} \bar{E} [P(\bar{E}, \omega_c, R = \omega_c L) - P(\bar{E}, \omega_c, R_\chi = \chi^2 \omega_c L)] \end{aligned} \quad (17)$$

This calculation is straightforward since a finite emission angle Θ can be taken into account simply by reducing the kinematical constraint $k_\perp < \omega$ in (1) to $k_\perp < \chi \omega$, $\chi = \sin \Theta$. In Fig.3, we compare the resulting angular radiation patterns obtained in the single hard and multiple soft scattering approximation. In agreement with the discussion following eq.

(11) above, we find that for comparable sets of model parameters ω_c , R and $\bar{\omega}_c$, \bar{R} , $n_0 L$ respectively, the multiple soft and single hard scattering approximations lead to a comparable angular dependence of $\langle \Delta E \rangle(\Theta)$ for $\Theta > 10^\circ$. For smaller angles, deviations persist which one can understand quantitatively¹⁰ and which should be regarded as an intrinsic uncertainty of this calculation.

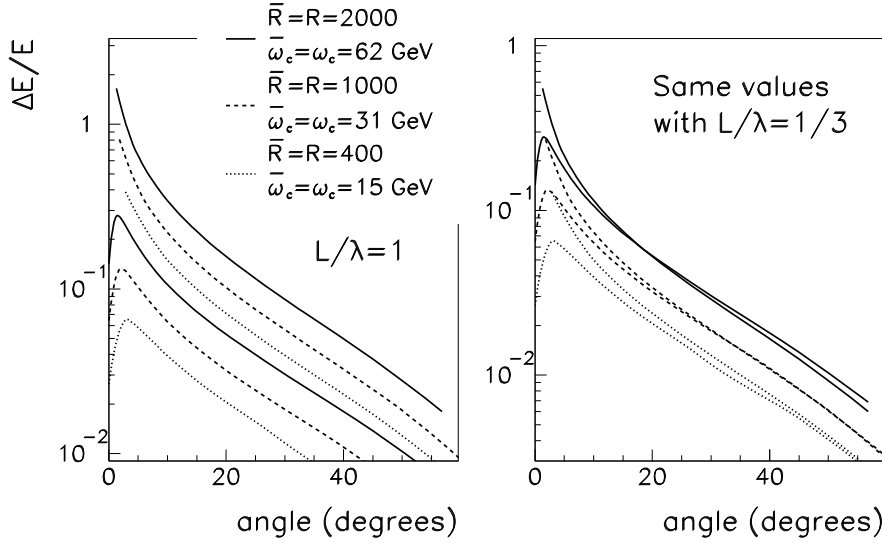


Figure 3. The average energy loss (17) radiated outside an angle Θ as calculated in the multiple soft (lower three lines) and single hard (upper three lines) scattering approximation. Fig. from Ref.¹⁰.

5. Application

The quenching weight $P(\Delta E)$ determines the quenching factor¹⁷

$$Q(p_\perp) = \int d\Delta E P(\Delta E) \left(\frac{d\sigma^{\text{vac}}(p_\perp + \Delta E)/dp_\perp^2}{d\sigma^{\text{vac}}(p_\perp)/dp_\perp^2} \right), \quad (18)$$

which determines the reduction of transverse momentum leading hadron spectra due to medium-induced energy loss. Alternatively, the quenching weight can be used to determine medium-modified fragmentation functions²⁰

$$D_{h/q}^{(\text{med})}(x, Q^2) = \int_0^1 d\epsilon P(\epsilon) \frac{1}{1-\epsilon} D_{h/q}\left(\frac{x}{1-\epsilon}, Q^2\right). \quad (19)$$

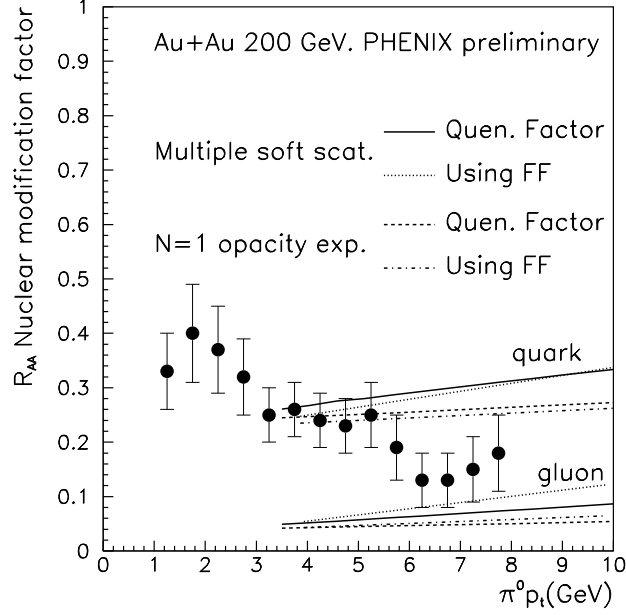


Figure 4. The nuclear modification factor for π^0 -production² compared to model calculations involving parton energy loss only. Curves present the quenching factor (18) and the suppression factor (20) obtained from medium-modified fragmentation functions. They are given in the limiting cases where all parent partons are either quarks (upper lines) or gluons (lower lines). Calculations in the multiple soft scattering approximation use $R = 2000$, $\omega_c = 67.5$ GeV, corresponding to $\hat{q} = 0.75 \frac{\text{GeV}^2}{\text{fm}}$ and $L = 6$ fm. In the single hard scattering approximation, we use $\bar{R} = R$, $\bar{\omega}_c = \omega_c$. Fig. from Ref. ¹⁰.

From these, the reduction of leading transverse momentum spectra can be calculated¹⁰ by convoluting with the perturbative hard matrix elements which are approximately proportional to x^6 ,

$$R_{ff}(p_\perp) = \frac{x_{\text{max}}^6 D_{h/q}^{(\text{med})}(x_{\text{max}}, p_\perp^2)}{x_{\text{max}}^6 D_{h/q}(x_{\text{max}}, p_\perp^2)} \bigg|_{p_\perp = x_{\text{max}} E_q}. \quad (20)$$

In Fig.4, we compare the data on the suppression of the π^0 -spectra to suppression factors calculated from (18) and (20). We find that both definitions of the suppression factors lead to quantitatively comparable re-

sults. Moreover, the single hard and multiple soft scattering approximation lead to quantitatively comparable results for suitable choices of the model parameters. Remarkably, we find that in the presence of kinematical constraints depleting the infrared region of $\omega \frac{dI}{d\omega}$ in Fig.1, the p_\perp -dependence of the quenching factor flattens considerably. This feature is necessary to find in Fig.4 a shallow p_\perp -dependence which is consistent with the data.

The application of the current calculations of parton energy loss to data below $p_\perp < 10$ GeV entails significant theoretical uncertainties. On the one hand, there are plausible competing physics effects which may be relevant at $p_\perp < 10$ GeV (see Ref.¹⁰ for further discussion). On the other hand, the high-energy “eikonal” approximation used in the derivation of (1) becomes questionable if $\Delta E \sim E$ which is the case in Fig.4. This should motivate improved calculations of (1) for which the finite energy effects of the partonic projectile are taken into account.

References

1. K. Adcox *et al.* [PHENIX Collaboration], Phys. Rev. Lett. **88** (2002) 022301.
2. S. Mioduszewski [PHENIX Collaboration], arXiv:nucl-ex/0210021.
3. C. Adler *et al.*, Phys. Rev. Lett. **89** (2002) 202301.
4. C. Adler *et al.* [STAR Collaboration], Phys. Rev. Lett. **90** (2003) 032301.
5. C. Adler *et al.* [STAR Collaboration], arXiv:nucl-ex/0210033.
6. E. Wang and X. N. Wang, Phys. Rev. Lett. **89** (2002) 162301.
7. M. Gyulassy, I. Vitev and X. N. Wang, Phys. Rev. Lett. **86** (2001) 2537.
8. B. Muller, arXiv:nucl-th/0208038.
9. T. Hirano and Y. Nara, arXiv:nucl-th/0301042.
10. C. A. Salgado and U. A. Wiedemann, arXiv:hep-ph/0302184.
11. R. Baier, Y. L. Dokshitzer, A. H. Mueller, S. Peigne and D. Schiff, Nucl. Phys. B **483** (1997) 291.
12. B. G. Zakharov, JETP Lett. **63** (1996) 952.
13. U. A. Wiedemann, Nucl. Phys. B **588** (2000) 303.
14. M. Gyulassy, P. Levai and I. Vitev, Nucl. Phys. B **594** (2001) 371.
15. U. A. Wiedemann, Nucl. Phys. A **690** (2001) 731.
16. R. Baier, Y. L. Dokshitzer, A. H. Mueller, S. Peigne and D. Schiff, Nucl. Phys. B **484** (1997) 265.
17. R. Baier, Y. L. Dokshitzer, A. H. Mueller and D. Schiff, JHEP **0109** (2001) 033.
18. C. A. Salgado and U. A. Wiedemann, Phys. Rev. Lett. **89** (2002) 092303.
19. F. Arleo, JHEP **0211** (2002) 044.
20. X. N. Wang, Z. Huang and I. Sarcevic, Phys. Rev. Lett. **77** (1996) 231.